Available online at www.sciencedirect.com
SCIENCE DIRECT
Geochimica et Cosmochimica Acta 70 (2006) 2311–2324
Geochimica
www.elsevier.com/locate/gca

Equation of state of the H_2O, CO_2, and H_2O–CO_2 systems up to 10 GPa and 2573.15 K: Molecular dynamics simulations with ab initio potential surface

Zhenhao Duan *, Zhigang Zhang

State Key Laboratory of Lithospheric Evolution, Institute of Geology and Geophysics, Chinese Academy of Sciences, Beijing, 100029, China

Received 21 November 2005; accepted in revised form 16 February 2006

Abstract

Based on our previous development of the molecular interaction potential for pure H_2O and CO_2 [Zhang, Z.G., Duan, Z.H. 2005a. Isothermal–isobaric molecular dynamics simulations of the PVT properties of water over wide range of temperatures and pressures. *Phys. Earth Planet Interiors* **149**, 335–354; Zhang, Z.G., Duan, Z.H. 2005b. An optimized molecular potential for carbon dioxide. *J. Chem. Phys.* **122**, 214507] and the ab initio potential surface across CO_2–H_2O molecules constructed in this study, we carried out more than one thousand molecular dynamics simulations of the *PVTx* properties of the CO_2–H_2O mixtures in the temperature–pressure range from 673.15 to 2573.15 K up to 10.0 GPa. Comparison with extensive experimental *PVTx* data indicates that the simulated results generally agree with experimental data within 2% in density, equivalent to experimental uncertainty. Even the data under the highest experimental temperature–pressure conditions (up to 1673 K and 1.94 GPa) are well predicted with the agreement within 1.0% in density, indicating that the high accuracy of the simulation is well retained as the temperature and pressure increase. The consistent and stable predictability of the simulation from low to high temperature–pressure and the fact that the molecular dynamics simulation resort to *no* experimental data but to ab initio molecular potential makes us convinced that the simulation results should be reliable up to at least 2573 K and 10 GPa with errors less than 2% in density. In order to integrate all the simulation results of this study and previous studies [Zhang and Duan, 2005a, 2005b] and the experimental data for the calculation of volumetric properties (volume, density, and excess volume), heat properties, and chemical properties (fugacity, activity, and possibly supercritical phase separation), an equation of state (EOS) is laboriously developed for the CO_2, H_2O, and CO_2–H_2O systems. This EOS reproduces all the experimental and simulated data covering a wide temperature and pressure range from 673.15 to 2573.15 K and from 0 to 10.0 GPa within experimental or simulation uncertainty.
© 2006 Elsevier Inc. All rights reserved.

1. Introduction

CO_2–H_2O is the most frequently encountered fluid mixtures in and around the Earth, widely existent in various geospheres, as revealed from direct measurements or from the study of fluid inclusions in various rocks and ore deposits (Roedder, 1984; Labotka, 1991). The functional relationship of pressure–volume–temperature-composition (the *PVTx* property) is the most fundamental thermodynamic property because it can be used to construct equations of state, which can in turn calculate volumetric properties (density, volume, and compressibility), phase behavior (immiscibility, phase equilibrium, and solubility), heat properties (enthalpy) and chemical properties (activity, fugacity, and chemical potential). *PVTx* property is also important in the analysis of fluid inclusions for tracing the formation conditions of geological bodies (Roedder, 1984; Bodnar, 1985; Ramboz et al., 1985; Labotka, 1991), in the study of mineral precipitation caused by the boiling of CO_2–H_2O fluid (Drummond and Ohmoto, 1985; Bowers,

* Corresponding author.
E-mail address: duanzhenhao@yahoo.com (Z. Duan).

0016-7037/$ - see front matter © 2006 Elsevier Inc. All rights reserved.
doi:10.1016/j.gca.2006.02.009

1991), in the investigation of mineral–rock interactions, and in the simulation of CO_2 sequestration (Haugan and Drange, 1992; Spycher and Pruess, 2005).

Over last half century, more than twenty research laboratories reported more than thirty data sets on the *PVTx* or volumetric properties of this binary (in Table 1). We projected these data in Fig. 1, which shows that the data are generally limited below 1000 K and 0.6 GPa, equivalent to the upper crust conditions. Only a small number of data points covering the temperature and pressure range up to 1673 K and 1.94 GPa, essentially no data applicable for the conditions in the lower crust and mantle, where there should exists large amounts of CO_2 and H_2O (Navon et al., 2004).

Although experimentalists are still devoting extensive efforts on the expanding of the database of this binary system in the *TP* space, their path to higher *T* and *P* conditions proves to be very difficult (Frost and Wood, 1997). It is unlikely in the near future that experiments can cover a wide *TP* space (say up to 2573.15 K and 10.0 GPa) in the measurement of the thermodynamic properties of this binary system. Scientists have been taking new approaches to investigate this binary system.

Equations of state (EOS) provide possible formalism to interpolate and extrapolate experimental data. Extensive

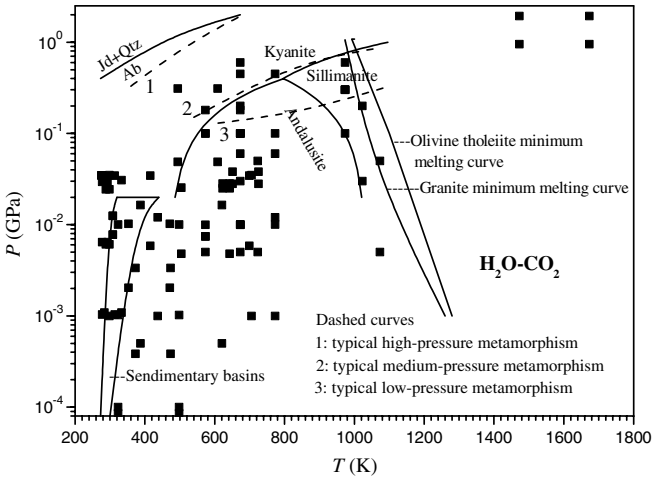

Fig. 1. The distribution of experimental *PVTx* data of the CO_2–H_2O system in *TP* space.

efforts have been devoted to develop such an EOS for the CO_2-H_2O binary system (Holloway, 1977; Kerrick and Jacobs, 1981; Bowers and Helgeson, 1983; Duan et al., 1992, 1996; Churakov and Gottschalk, 2003). However, none of these can predict the properties over a wide temperature and pressure range. The EOS of Duan et al. (1992) is the

Table 1
The experimental *PVTx* properties of the CO_2–H_2O system

Authors	*T* (K)	*P* (MPa)	Concentration	N_d
Ohsumi et al. (1992)	276.15	34.754	$x(CO_2)\% = 0.1798–0.6294$	5
Teng et al. (1997)	278–293	6.44–29.49	$x(CO_2)\% = 2.50–3.49$	24
Parkinson and De Nevers (1969)	278.1–313.7	1.0342–34.4744	$x_{CO_2}\%$ (mol) = 0.1–2.2	28
Hebach et al. (2004)	283.80–333.19	1.09–30.66	$x(CO_2)$ = saturated values	201
King et al. (1992)	288.15–298.15	6.08–24.32	$x(CO_2)\% = 2.445–3.070$	27
Hnedkovsky et al. (1996)	298.15–705.38	1–35	$m(CO_2) = 0.155–0.185$	32
Zhang et al. (2002)	308.15	7.752–12.484	$x(CO_2)\% = 0.3$	16
Patel et al. (1987)	323.15–498.15	0–10	$x(CO_2) = 0.5–0.98$	457
Patel and Eubank (1988)	323.15–498.15	0.0855–1.0237	$x(CO_2) = 0.02–0.5$	297
Nighswander et al. (1989)	352.85–471.25	2.04–10.21	$x(CO_2)\% = 0.22–1.66$	33
Zawisza and Malesinska (1981)	373.15–473.15	0.385–3.35	$y(H_2O) = 0.1210–0.9347$	145
Ellis (1959)	387.15–621.15	0.5–16.4	$y(CO_2)\% = 3.90$-6.27–84.02	36
Fenghour et al. (1996)	415.36–699.30	5.884–34.577	$x(CO_2) = 0.0612–0.7913$	164
Wormald et al. (1986)	437.2–773.2	1–12	$x(CO_2) = 0.5$	115
Sterner and Bodnar (1991)	494.15–608.15	48.7–310	$x(CO_2) = 0.1234–0.7473$	84
	673.15–973.15	100–600	$x(CO_2) = 0.1234–0.8736$	107
Ellis and Golding (1963)	504.15–643.15	4.791–25.443	[b]	9
Singh et al. (2000)	573.15	7.44–99.93	$x(CO_2) = 0.05–0.9$	58
Seitz and Blencoe (1997)	573.15–673.15	9.94–99.94	$x(CO_2) = 0.1–0.9$	113
Zakirov (1984)	573.15–673.15	5–180	$x(CO_2) = 0.2–0.805$	149
Zhang and Frantz (1992)	519.95–634.45	[a]	$x(CO_2)\% = 5.5–16.5$	29
Crovetto and Wood (1992)	622.75–642.70	19.64–28.13	$x(CO_2)\% = 0.48–0.8745$	72
Crovetto et al. (1990)	651.10–725.51	27.98–38.05	$x(CO_2)\% = 0.130–1387$	94
Seitz and Blencoe (1999)	673.15	9.94–99.93	$x(CO_2) = 0.1–0.9$	95
Gehrig (1980)	673.15–773.15	10–60	$x(CO_2) = 0.1–0.9$	198
Shmulovich et al. (1980)	673.15–773.15	100–450	$x(CO_2) = 0.087–0.6232$	33
Franck and Todheide (1959)	673.15–1023.15	30–200	$x(CO_2) = 0.2–0.8$	303
Greenwood (1969)	723.15–1073.15	5–50	$x(CO_2) = 0.1–0.9$	711
Frost and Wood (1997)	1473.15–1673.15	950–1940	$x(CO_2) = 0.108–0.787$	19

Note. N_d, number of data points; *x*, *y*, mole fraction; *m*, molality.
[a] Pressures are not reported, but can be calculated from their empirical formulations.
[b] Concentrations are not directly reported, but can be calculated from the report.

only one to be able to predict both *PVTx* properties and phase equilibrium, but is limited below about 0.2–0.3 GPa. The EOS of Duan et al. (1996) is purely a theoretical derivation from corresponding principle based on the assumption of spherical molecules and, according to current study, it contains errors up 9%. The other EOS's are only for pressures well below 1.0 GPa with considerable uncertainties.

In recent years, molecular level computer simulation (MLCS) emerges as an alternative approach for studying thermodynamic properties of geological fluids for the following reasons besides the reason of increasingly more powerful computers: (1) MLCS depends little on experimental data. Although molecular interaction potential is crucial in the simulation, the parameters of it are generally evaluated from a few data points in a small *TP* space or from ab initio calculations. Once the potential model is well established, it can be used to predict various thermodynamic, transport and liquid structure properties in a wide *TP* range; (2) Through MLCS, we can look into microscopic properties, which are generally difficult to observe experimentally; (3) There is no limitation on temperature, pressure and medium conditions, as long as the molecule does not change its elements. Therefore, MLCS is especially suitable for the study of the Earth and planets at extreme *TP* conditions.

The predictability of MLCS has been demonstrated by our recent work (Zhang and Duan, 2005a,b). We found through extensive comparison of our simulation results with experimental data that a molecular potential determined under room temperature and pressure can be used to predict *PVT* properties of H_2O up to 1873.15 K and 5.0 GPa with remarkable accuracy (Zhang and Duan, 2005a). We believe the predictability can be extended up to 20 GPa, because the accuracy in predicted density increases with pressure: from 0.1 to 5.0 GPa the errors decrease from about 2% to less than 1%. We have also developed a potential surface of CO_2 (Zhang and Duan, 2005b) that simultaneously reproduces all the thermodynamic data of CO_2, including *PVT*, phase equilibrium, enthalpy, saturation pressure, and critical point in a wide temperature–pressure range.

With the previous work on H_2O and CO_2 as basis, we make a further effort to investigate the *PVTx* properties of CO_2–H_2O system over wide *TP* range with molecular dynamics simulations in this study. The crucial issue for the simulations of the mixture is to find the unlike interaction potential between the water molecules and carbon dioxide molecules. Since we adopt similar site–site models with partial charges for both the CO_2 and H_2O molecules, it is possible to parameterize the cross interaction potential with different combining rules. We first tried the conventional Lorentz–Berthelot combining rule and the widely used Kong combining rule (Kong, 1973) and found that they are not able to accurately predict the non-ideal behavior of the mixture. We took an alternative approach to parameterize the cross mixing potential through non-linear fitting to the ab initio potential surface and proved that it substantially improves the prediction for the non-ideal mixing property. Our simulations, as will be shown later, would reproduce experimental data with remarkable accuracies. Based on the simulated data and experimental data, an EOS is developed, which we believe is the most accurate up to date for this mixture in the range from 673.15 to 2573.15 K and from 0 to 10.0 GPa.

In the following section, we will present the simulation details, including the potential models, simulation algorithms and setups. The simulation results will then be discussed in detail, followed by the presentations of an equation of state. Finally, some conclusions will be drawn.

2. Simulation details

In this study, we carried out more than one thousand isothermal–isobaric molecular dynamics simulations with algorithms proposed in our previous paper (Zhang and Duan, 2005a). We briefly describe the potential models, simulation algorithms, and computational details below.

2.1. Potential models

Interaction potentials of molecules play key roles in the molecular level simulation. There are three kinds of molecular interactions involved in the CO_2–H_2O system: H_2O–H_2O, CO_2–CO_2, and CO_2–H_2O interactions. We have extensively searched for H_2O–H_2O potential and found that SPC/E potential can accurately predict *PVT* properties at least up to 5 GPa and possibly up to 20 GPa (Zhang and Duan, 2005a). We also optimized a potential for CO_2–CO_2 which shows excellent predictability and transferability illustrated in our previous paper (Zhang and Duan, 2005b). Based on the formula for H_2O–H_2O and CO_2–CO_2 potentials, the following form is proposed for the CO_2–H_2O potential:

$$u(1,2) = u_{\text{short}}(1,2) + u_{\text{Coul}}(1,2) = \sum_{i\in\{1\}}\sum_{j\in\{2\}} 4\varepsilon_{ij}\left[\left(\frac{\sigma_{ij}}{r_{ij}}\right)^{12} - \left(\frac{\sigma_{ij}}{r_{ij}}\right)^{6}\right] + \sum_{i\in\{1\}}\sum_{j\in\{2\}}\frac{q_i q_j}{r_{ij}}, \tag{1}$$

where r_{ij} is the distance between the interaction sites; q_i and q_j are the partial charges designated on the interaction sites; ε_{ij} and σ_{ij} are the energy and size parameters for the short-range Lennard-Jones potential, which can be parameterized from two routines: combining rules or non-linear fitting to ab initio potential surface. The procedures of parameterizations are briefly described as follows.

2.1.1. Parameterization with combining rules

The conventional Lorentz–Berthelot combining rule is used widely for its simplicity:

$$\varepsilon_{ij} = \sqrt{\varepsilon_{ii}\varepsilon_{jj}}, \tag{2}$$

Table 2
The interaction potential parameters between CO_2 and H_2O

Partial charges						
CO_2	C	0.5888	O	−0.2944		
H_2O	H	0.4238	O	−0.8476		
	Lorentz–Berthelot		Kong		Ab initio	
	ε/k_B (K)	σ (Å)	ε/k_B (K)	σ (Å)	ε/k_B (K)	σ (Å)
Short-range interaction parameters						
$C–O_{(H_2O)}$	47.494	2.9789	44.713	3.0031	35.240	3.1156
$O_{(CO_2)}–O_{(H_2O)}$	80.397	3.0830	80.127	3.0836	63.996	3.0297
C–H	—	—	—	—	36.049	2.8142
$O_{(CO_2)}$–H	—	—	—	—	47.185	2.1942

$$\sigma_{ij} = (\sigma_{ii} + \sigma_{jj})/2. \tag{3}$$

Another combining rule discussed here is proposed by Kong and is considered to be superior to Lorentz–Berthelot combining rule for accurate predictions of equilibrium properties (Delhommelle and Mille, 2001). Kong combining rule can be expressed with the following equations (Kong, 1973):

$$\varepsilon_{ij}\sigma_{ij}^{12} = (\varepsilon_{ii}\sigma_{ii}^{12}/2^{13})[1 + (\varepsilon_{jj}\sigma_{jj}^{12}/\varepsilon_{ii}\sigma_{ii}^{12})^{1/13}]^{13}, \tag{4}$$

$$\varepsilon_{ij}\sigma_{ij}^{6} = (\varepsilon_{ii}\sigma_{ii}^{6}\varepsilon_{jj}\sigma_{jj}^{6})^{1/2}. \tag{5}$$

The parameters determined from Eqs. (2)–(5) are listed in Table 2.

2.1.2. Parameterization by non-linear fitting to ab initio potential surface

In the last two decades, the ab initio potential surface of CO_2–H_2O dimer has been studied by several research groups (Mehler, 1981; Hurst et al., 1986; Block et al., 1992; Makarewicz et al., 1993; Kieninger and Ventura, 1997; Sadlej et al., 1998). There are some differences between the results of different researchers. The ab initio calculations of Sadlej et al. (1998) were chosen after we examined these studies carefully. Firstly, the work of Sadlej et al. (1998) employed both the extended basis sets and the BSSE (basis set superposition error) correction of interaction energies that was neglected by most of other researchers. Thus, their results should be more accurate. Secondly, the studies of the potential energy surface given by Sadlej et al. (1998) are more extensive and detailed than others, including more configurations and data points.

In order to calculate the potential surface of CO_2–H_2O complex, we establish the same system of coordinates proposed by Sadlej et al. (1998), as shown in Fig. 2. The z-axis of the system is chosen passing through the center the oxygen atom of a water molecule and the center of carbon atom of a carbon dioxide molecule while the origin is located at the midpoint between these two centers. The plane of the water molecule determines the xz-plane. In this system of coordinates, configurations of CO_2–H_2O complex can be described with four quantities: the distance r between the oxygen atom and carbon atom, the angle θ between CO_2 and the z-axis, the angles τ_1 and τ_2 which describe the out-of-plane torsion and the in-plane wagging of H_2O about CO_2, respectively.

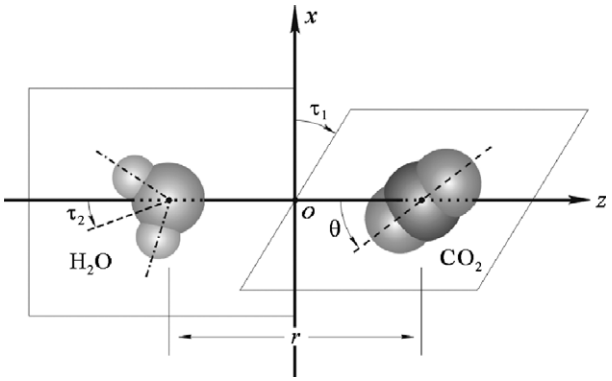

Fig. 2. The system of coordinates established for the calculation of CO_2–H_2O potential surface.

Multidimensional simplex non-linear fitting method was adopted in our parameterization (Nelder and Mead, 1965). Ab initio calculation results were provided by Dr. Sadlej through personal communication. The short-range interactions contributed from hydrogen atoms can not be neglected and become significant for the configurations with τ_2 larger than 90°. Consequently, the Lennard-Jones parameters related to hydrogen atoms were included in the fitting procedure and this involves eight non-linear parameters in total. In the course of parameterization, the optimization was repeated with different initial configurations to decrease the possibility of local minimum. Non-linear fitted potential with the parameters listed in Table 2 is compared to the ab initio calculation results with several typical configurations in Fig. 3, which shows that the fitted result is satisfying.

2.2. Simulation algorithms and setups

Based on the motion equations of Martyna et al. (1994), the following equations of motion were adopted to propagate the MD trajectories with the isothermal–isobaric ensemble.

$$\ddot{\mathbf{r}}_i = \mathbf{F}_i/m_i + \dot{\eta}^2\mathbf{r}_i + \ddot{\eta}\mathbf{r}_i - (\xi + 3\dot{\eta}/f)(\dot{\mathbf{r}}_i - \dot{\eta}\mathbf{r}_i), \tag{6a}$$

$$\ddot{\eta} = (P_{\text{inst}} - P_{\text{desire}})\exp(3\eta)/t_p^2 k_B T_{\text{desire}} + \sum_{i=1}^{N} m_i(\dot{\mathbf{r}}_i - \dot{\eta}\mathbf{r}_i)^2/f t_p^2 k_B T_{\text{desire}} - \xi\dot{\eta}, \tag{6b}$$

$$\dot{\xi} = \left[\sum_{i=1}^{N} m_i(\dot{\mathbf{r}}_i - \dot{\eta}\mathbf{r}_i)^2 + 3\dot{\eta}^2 t_p^2 k_B T_{\text{desire}} - (f+1)k_B T_{\text{desire}}\right] \Big/ Q, \tag{6c}$$

$$\eta = \ln V^{1/3}, \tag{6d}$$

where $\mathbf{r}_i$, $\mathbf{F}_i$, and m_i are the position, force and mass of the ith particle, respectively; ξ and η are the thermostat and barostat variables, with two corresponding parameters of

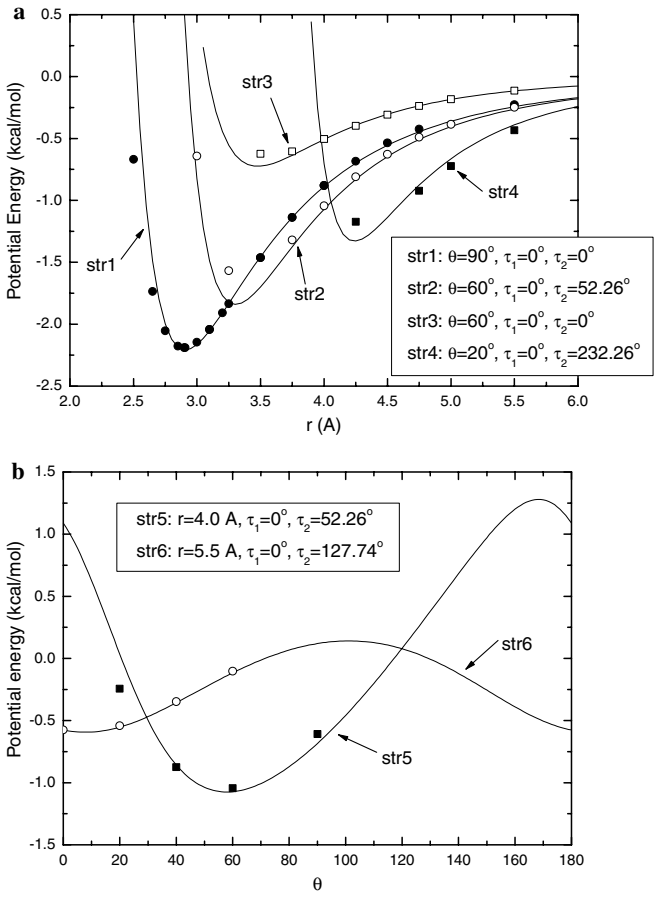

Fig. 3. The non-linear fitted potential of CO_2–H_2O (solid line) from the ab initio calculation results of Sadlej et al. (1998) (discrete point). (a) The variation of interaction potential with distance r; (b) The variation of interaction potential with angle θ.

Q and t_p to adjust the fluctuation of temperature and pressure; V is the volume; f is the degree of freedom of the simulated system with N particles; k_B is the Boltzmann constant; P_{desire} and T_{desire} are the desired/external pressure and temperature; P_{inst} is the instantaneous pressure, which is calculated from atomic virial $W = \frac{1}{3}\sum_i \mathbf{F}_i \cdot \mathbf{r}_i$ (Martyna et al., 1994):

$$P_{inst} = \frac{1}{3V}\sum_{i=1}^{N} m_i(\dot{\mathbf{r}}_i - \dot{\eta}\mathbf{r}_i)^2 + \frac{W}{V}. \quad (7)$$

Eq. (6) has an apparently different form from that presented in Martyna et al. (1994) but can easily found to be entirely equivalent with mathematical transformations of $\dot{\xi} = \frac{p_\xi}{Q} \Rightarrow \xi$, $\frac{p_\eta}{W} \Rightarrow \dot{\eta}$, and $W \Rightarrow 3t_p^2 k_B T_{desire}$ from their Eq. (2.9). According to our experience, despite the equivalence, Eq. (6) is more straightforward and convenient to integrate the molecular dynamics trajectory than Martyna's algorithm, as shown in detail in our previous publication (Zhang and Duan, 2005a). In addition, since the confusing velocity of particle $\mathbf{v}_i = \dot{\mathbf{r}}_i - \dot{\eta}\mathbf{r}_i$ is not involved in our equations of motion, the original description of RATTLE constraint dynamics algorithm (Andersen, 1983) can be directly used without any further modifications, which is also much simpler than Martyna's algorithm.

In all of our molecular dynamics simulations, at least 256 molecules were placed in a cubic simulation box and the number of each component in the mixture was set to be larger than 20 to ensure the statistical reliability. When comparing with experiments, the number of each component was adjusted to precisely pinpoint the corresponding experimental composition. The conventional periodic boundary conditions and minimum image conventions were used in the simulations to calculate inter-atom distances (Allen and Tildesley, 1989). Long-range electrostatic forces and energies were calculated with the Ewald summation. Long-range corrections to the Lennard-Jones interactions were made with the formulations presented by Zhang and Duan (2002). Velocity Verlet algorithm (Swope et al., 1982) was adopted to propagate the statistical trajectory, which was described in detail in the Appendix of Zhang and Duan (2005a). The geometries of CO_2 molecules were constrained with the RATTLE method (Andersen, 1983). The oxygen atoms were set as primary atoms in the propagation of MD trajectory and the positions of the carbon atoms were calculated as the midpoint of the other two oxygen atoms. Note that the forces acting on the carbon atoms should be carefully transformed to the primary oxygen atoms for consistence as suggested by Ciccotti et al. (1982). Parameters of Q and t_p in Eq. (6) were adjusted to control the fluctuation of temperature and pressure according to the suggestion of Martyna et al. (1994), with a typical value of 5.0 kJ ps^2/mol for Q and 5.0 ps for t_p. The time step of all the simulations was set as 1.0 fs. Simulations were initiated from the configurations "melted" from the face-centered cubic lattice structure or the previous equilibrated configurations at similar densities. The instantaneous volumes were recorded and counted into the statistical average for about 50 ps after a 10–20 ps pre-equilibrium simulation. At lower temperatures and higher pressures, longer simulations (to 80 ps) were performed to ensure the convergence of the simulation and sufficient statistical reliability.

As discussed in our previous paper (Zhang and Duan, 2005a), we carefully checked the possible finite-size effect and the adequacy of the simulation lengths. Little differences were found when the system size is increased from 256 to 512 molecules. As the total simulation time is increased from 50–80 to 200 ps, the simulation results of volumetric and structural properties were almost identical. So we conclude that our choice of the system size and simulation length should be appropriate.

3. Simulation results and discussions

3.1. Comparisons with experiments

Seitz and Blencoe (1999) measured the densities of CO_2–H_2O mixture through a well-established vibrating-tube

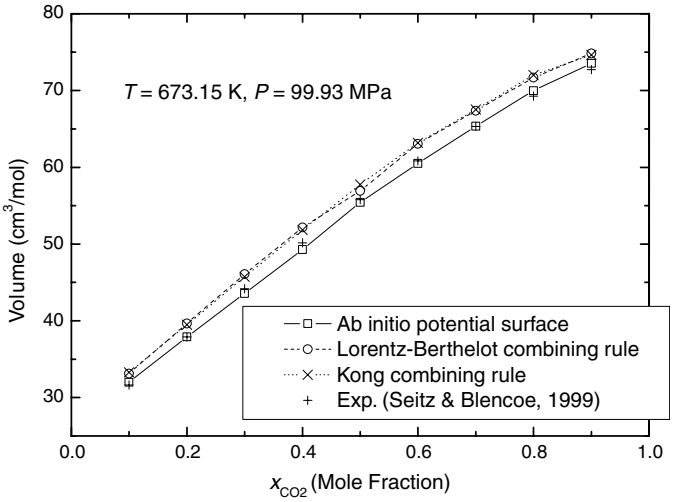

Fig. 4. Comparisons between the experiments of Seitz and Blencoe (1999) and MD simulation results of this study with different parameters at 673.15 K and 99.93 MPa. The uncertainty of each simulation data is around the size of the corresponding symbol.

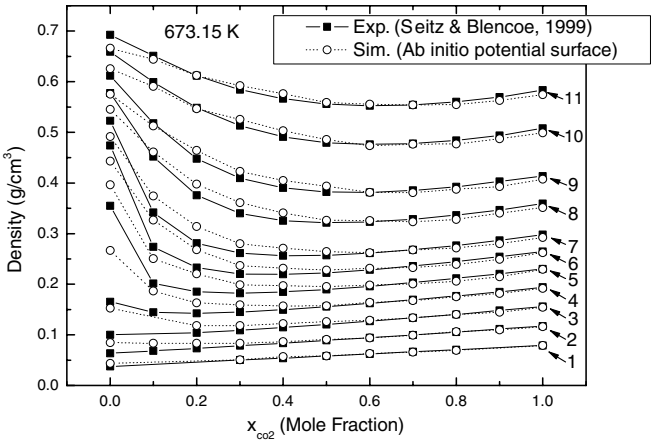

Fig. 5. Comparisons between the densities from the measurements of Seitz and Blencoe (1999) and MD simulations of this study with ab initio potential surface at 673.15 K. Experimental densities of pure water ($x_{CO_2} = 0$) are calculated with the accurate EOS of Wagner and Pruß (2002). The experimental data are linked with solid lines and simulated densities are linked with dotted lines for clarity. The numbers near the tails of arrows represent the eleven pressures of the isobaric curves: 1: 9.94 MPa; 2: 14.94 MPa; 3: 19.94 MPa; 4: 24.94 MPa; 5: 29.94 MPa; 6: 34.94 MPa; 7: 39.94 MPa; 8: 49.93 MPa; 9: 59.93 MPa; 10: 79.93 MPa; and 11: 99.93 MPa.

densimeter at 673.15 K from 9.94 to 99.93 MPa, which we consider highly accurate. Fig. 4 shows the comparisons between the experiments of Seitz and Blencoe (1999) and our simulation results with different mixing parameters at 673.15 K and 99.93 MPa. The simulated volumes with the Lorentz–Berthelot and Kong combining rules are found to be comparable with each other, but systematically larger than the corresponding experimental data by 3.6–4.0%. On the other hand, the simulation results with ab initio potential surface agree well with experiments with an averaged deviation of 0.8% and maximum deviation of about 1.7%. Complete comparisons between all the experimental densities of Seitz and Blencoe (1999) and simulation results with ab initio potential surface are shown in Fig. 5, which shows that simulations agree well with the experimental measurements. The noticeable deviations of water-rich fluids at low pressures can attribute to the decreased accuracies of SPCE model at low pressures at 673.15 K, as shown in Fig. 2 of our previous paper (Zhang and Duan, 2005a). At higher pressures the SPCE model gives an increasingly accurate prediction of the volumetric property of water and good predictabilities are expected.

Shmulovich et al. (1980) and Sterner and Bodnar (1991) provide experimental $PVTx$ data under high pressures. As shown in Fig. 6, the combining rules of Lorentz–Berthelot and Kong overestimate the volumes with similar systematical deviations. Ab initio potential surface reproduces experimental volumes within 1.0% for most cases. Two data points seem to be not as accurate with deviations of -3.18 cm^3/mol (-5.9%) and $+0.98$ cm^3/mol (3.4%) at 100 and 500 MPa, respectively. We notice that the authors established an EOS based on their measured data (Shmulovich et al., 1980). Clear deviations of about -3.0 cm^3/mol and $+1.0$ cm^3/mol at these two data points with their

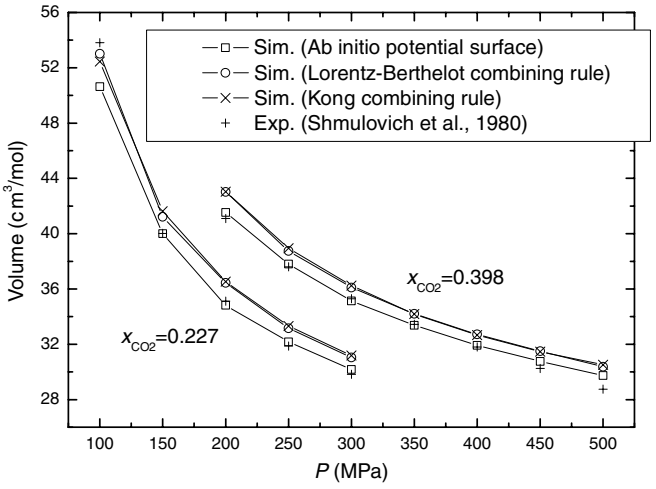

Fig. 6. Comparisons between the experiment of Shmulovich et al. (1980) and the MD simulation results of this study with different parameters at 773.15 K. The uncertainties of the simulated data are around the sizes of the symbols.

EOS are displayed in their Fig. 5(b), which implies the uncertainties of these two measured values.

In Figs. 4 and 6, the differences between simulation results with Lorentz–Berthelot and Kong combining rules are indistinguishable within the simulation uncertainties. This suggests that the parameters from these two combining rules are not quite distinct from each other within the uncertainties of the simulated $PVTx$ properties. Therefore, in the following discussions we would not show the simulation results with Kong combining rule for clarity.

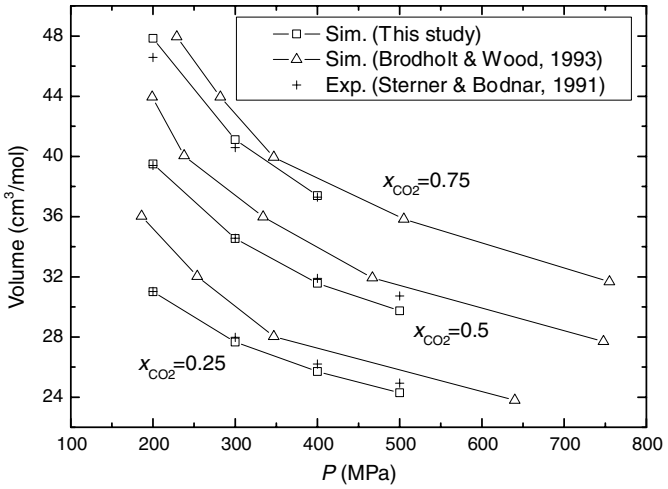

Fig. 7. The MD simulated volumes in this study and those simulated by prior workers (Brodholt and Wood, 1993) at 673.15 K compared with experimental results of Sterner and Bodnar (1991). The uncertainties of the simulation in this study are around the sizes of the symbols.

Brodholt and Wood (1993) attempted to study the $PVTx$ properties of CO_2–H_2O with TIP4P model for water and MSM3 model for carbon dioxide. They applied the Lorentz–Berthelot combining rule for the unlike CO_2–H_2O interactions. In order to compare with experimental data, additional interpolations are needed for their implementation of simple NVE molecular dynamics simulations. Fig. 7 shows that our simulation results are in significantly better agreement with experimental data of Sterner and Bodnar (1991) than Brodholt and Wood (1993). This is expected since the inter-molecular potentials we used for pure H_2O and CO_2 give better predictions than TIP4P and MSM3 adopted by Brodholt and Wood (1993). In the mean time, the potential between CO_2 and H_2O molecules obtained from ab initio surface further improved the accuracies.

The excess volume is calculated with the following equation:

$$V^{ex} = V_{mixture} - x_{CO_2} V_{CO_2} - (1 - x_{CO_2}) V_{H_2O}, \quad (8)$$

where $V_{mixture}$ is the molar volume of the mixture, x_{CO_2} is the mole fraction of carbon dioxide, V_{CO_2} and V_{H_2O} are molar volumes of pure carbon dioxide and water at the same TP condition. As shown in Fig. 8, simulated excess volumes with ab initio potential surface are systematically lower than those with Lorentz–Berthelot combining rule and are in significantly better agreement with experimental observations. From Fig. 8a, the experimental excess volumes by Shmulovich et al. (1980) are larger than those by Sterner and Bodnar (1991) in general and our simulations with ab initio potential surface agree well with the data of Shmulovich et al. (1980) within the uncertainties. Destrigneville et al. (1996) established an EOS for the excess volumes based on their Monte Carlo simulation results. We include their predictions at 773.15 K and 200.0 MPa in Fig. 8a, which shows their large overestimations as compared with the two sets of simulation data in this study. Fig. 8b and Fig. 8c show the simulated excess volumes in this study and comparisons with the data of Sterner and Bodnar (1991) at higher temperatures and pressures. Similar trends as Fig. 8a can be found and overall good agreements are found between the predictions with ab initio potential surface and experiments.

Frost and Wood (1997) provided the measured $PVTx$ properties of CO_2–H_2O under the highest temperatures and pressures up to now. We carried out MD simulations corresponding to the conditions of their measurements. As revealed by the data listed in Table 3, our simulations with ab initio potential surface are systematically more accurate than those with the combining rules. In order to clearly show the agreements of simulations with experiments, we project the simulated data with ab initio potential surface along with corresponding experimental data in Fig. 9. All of the simulation results are in remarkable agreement within the experimental uncertainties except the data point at $T = 1473.15$ K, $P = 950$ MPa, and $x_{CO_2} = 0.787$. Nevertheless, as shown in Fig. 9, the measured data at this point obviously deviates from the thermodynamic trend of the other points at the same TP condition. In the mean time, we notice that the authors claimed the difficulty in their measurement of CO_2-rich fluids and noticeable uncertainty at 950 MPa. So it is reasonable to conclude that the volume at this point is underestimated by the measurement of Frost and Wood (1997). The remarkable agreements shown in Table 3 and Fig. 9 demonstrate the predictability of our simulations.

3.2. Predictions

The comparisons described above indicate that our simulations with ab initio potential surface reproduce accurately the experimental data and show remarkable predictability for the $PVTx$ properties of CO_2–H_2O system. Especially, as the temperature and pressure increase, the predictability remains convincing. Accordingly, we extend our simulations from the experimental range (less than 1673.15 K and 2.0 GPa) to 10.0 GPa and 2573.15 K and present the simulated results (690 simulations for mixtures) in the electronic annex EA-1 (also available from www.geochem-model.org/programs.htm). We believe that these data should be accurate with uncertainties less than 2% in density, and should be confirmed by future experiments.

4. Equation of state of H_2O, CO_2, and H_2O–CO_2

In order to facilitate the applications in geochemistry, a number of equations of state have been proposed for the CO_2–H_2O system (Holloway, 1977; Kerrick and Jacobs, 1981; Bowers and Helgeson, 1983; Duan et al., 1992; Duan et al., 1996; Churakov and Gottschalk, 2003). Generally, these equations are empirically calibrated according to the available experimental data and the applicable range

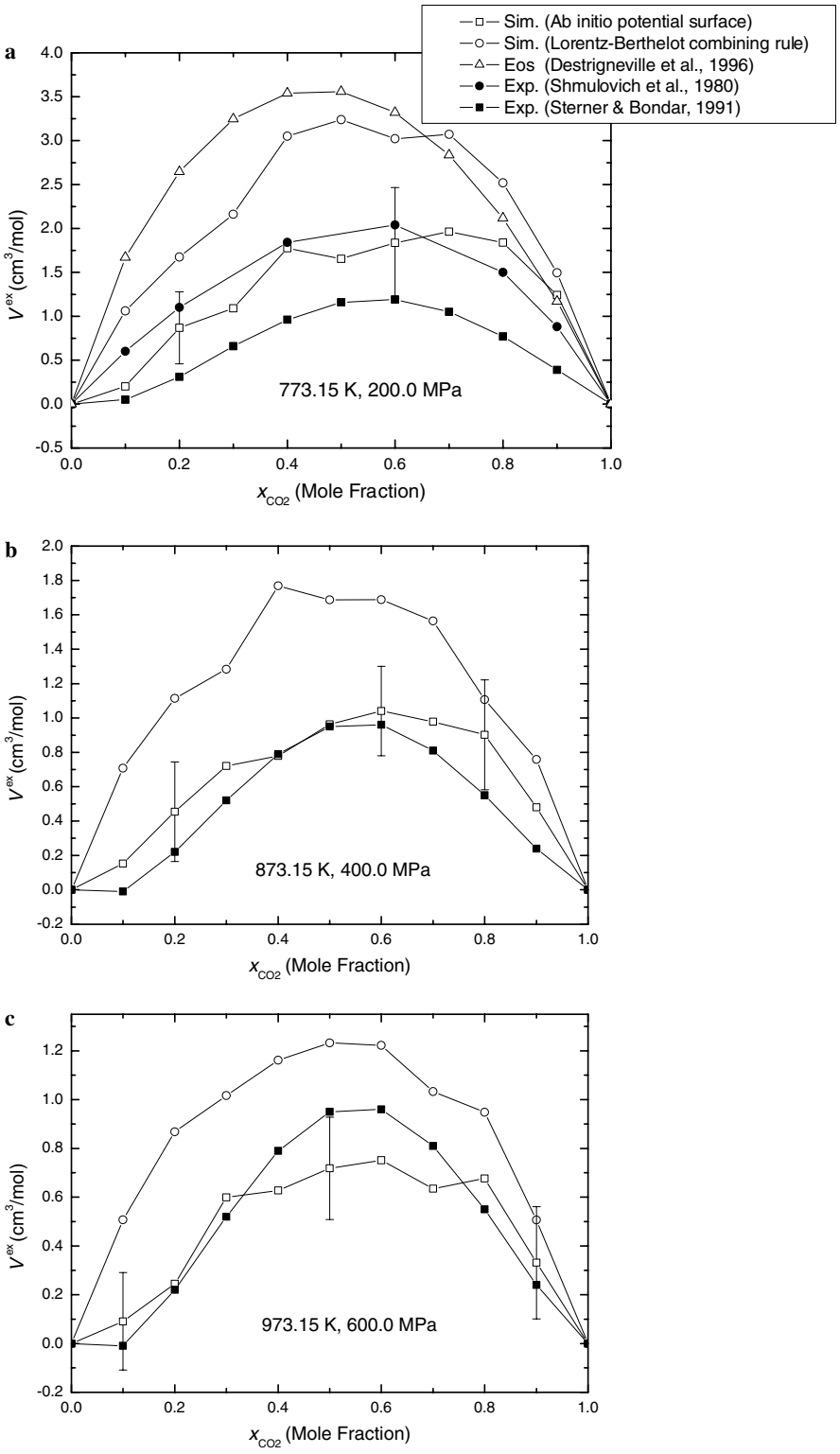

Fig. 8. Experimental excess volumes of Sterner and Bodnar (1991) and Shmulovich et al. (1980) and simulated excess volumes in this study with ab initio potential surface and Lorentz–Berthelot combining rule. Predictions by Destrigneville et al. (1996) are also included for comparisons. Representative uncertainties are marked with error bars at corresponding simulation data.

is well below 1.0 GPa. The EOS of Duan et al. (1996) is the only one derived from theory for the pressures well above 1.0 GPa. As compared with the simulation data listed in the electronic annex EA-1, this EOS gives underestimations of about 9.0% in density at $T = 1773.15$ K, $P = 10.0$ GPa, and $x_{CO_2} = 0.75$. With the reliable simulation results and new experimental data, it is now possible and necessary to develop an EOS to integrate all the data covering a wide temperature and pressure range with or close to experimental accuracy.

Table 3
Comparison of simulation results in this study with experimental volumes of Frost and Wood (1997)

T (K)	P (MPa)	x_{CO_2}	$V_{\text{ab initio}}$ (cm^3/mol)	V_{LB} (cm^3/mol)	V_{exp} (cm^3/mol)
1473.15	950	0.218	29.78(.09)	30.00(.14)	29.07(.73)
1473.15	950	0.413	33.55(.13)	33.88(.15)	32.95(.78)
1473.15	950	0.606	37.10(.12)	37.41(.09)	36.47(.83)
1473.15	950	0.787	40.28(.12)	40.46(.11)	38.63(.78)
1373.15	1450	0.146	23.19(.09)	23.30(.06)	23.09(.29)
1473.15	1450	0.226	25.40(.07)	25.52(.09)	25.37(.32)
1473.15	1450	0.297	26.58(.05)	26.79(.08)	26.61(.34)
1573.15	1450	0.128	24.39(.05)	24.47(.08)	24.31(.35)
1573.15	1450	0.149	24.74(.05)	24.83(.08)	24.5(.35)
1573.15	1450	0.205	25.71(.08)	25.87(.07)	25.51(.41)
1573.15	1450	0.289	27.20(.08)	27.41(.10)	26.82(.34)
1573.15	1450	0.387	28.96(.06)	29.09(.06)	28.61(.41)
1673.15	1450	0.237	27.07(.11)	27.19(.11)	26.78(.48)
1673.15	1450	0.39	29.72(.08)	29.88(.09)	29.65(.48)
1673.15	1450	0.45	30.72(.07)	30.84(.09)	30.37(.46)
1673.15	1940	0.175	23.26(.06)	23.27(.05)	23.27(.22)
1673.15	1940	0.21	23.84(.07)	23.98(.03)	23.98(.25)

Note. x_{CO_2} is the mole fraction of carbon dioxide, $V_{\text{ab initio}}$ is the simulated volume in this study with ab initio potential surface, V_{LB} is the simulated volume with Lorentz–Berthelot combining rule, the numbers in the parenthesis are the uncertainties of corresponding volumes.

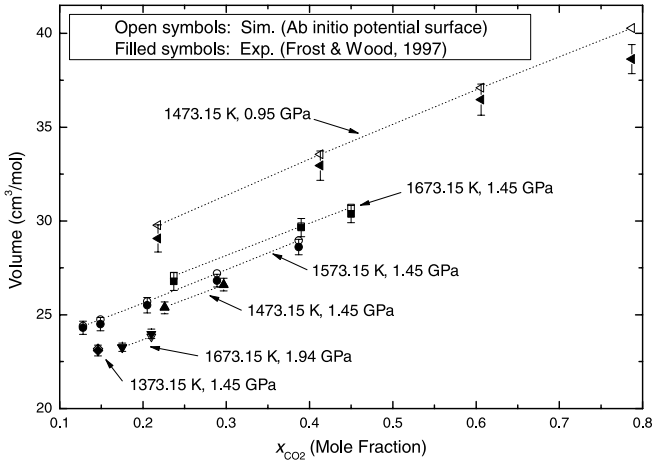

Fig. 9. Comparisons between the experimental volumes of Frost and Wood (1997) and corresponding simulation results of this study with ab initio potential surface. Filled symbols with error bars are experimental data and open symbols connected with dotted lines are simulated volumes.

The EOS proposed in this study is taken from Duan et al. (1992):

$$Z = \frac{PV}{RT} = 1 + \frac{BV_c}{V} + \frac{CV_c^2}{V^2} + \frac{DV_c^4}{V^4} + \frac{EV_c^5}{V^5} + \frac{FV_c^2}{V^2} \times \left(\beta + \frac{\gamma V_c^2}{V^2}\right) \exp\left(-\frac{\gamma V_c^2}{V^2}\right), \quad (9)$$

where $R = 83.14467$ cm^3 bar/(K mol) is the universal gas constant. For the end-members, the parameters $(B, C, D, \ldots)$ in Eq. (9) are calculated with the following equations:

$$B = a_1 + \frac{a_2}{T_r^2} + \frac{a_3}{T_r^3}, \quad (10a)$$

$$C = a_4 + \frac{a_5}{T_r^2} + \frac{a_6}{T_r^3}, \quad (10b)$$

$$D = a_7 + \frac{a_8}{T_r^2} + \frac{a_9}{T_r^3}, \quad (10c)$$

$$E = a_{10} + \frac{a_{11}}{T_r^2} + \frac{a_{12}}{T_r^3}, \quad (10d)$$

$$F = \frac{\alpha}{T_r^3}, \quad (10e)$$

$$T_r = \frac{T}{T_c}, \quad (10f)$$

$$V_c = \frac{RT_c}{P_c}, \quad (10g)$$

where T_c and P_c are the critical temperature and critical pressure respectively. For water, $T_c = 647.25$ K and $P_c = 221.19$ cm^3/mol. While for carbon dioxide, $T_c = 304.1282$ K and $P_c = 73.773$ cm^3/mol.

Additional 15 parameters in Eqs. (9) and (10) for each end-member are determined by fitting to over 2500 available experimental data and the simulation volumes. In order to optimize the EOS, the whole TP range is divided into two sub-regions with 200 MPa as the switching boundary (Table 4). Compared with the well-known IAPWS95 model (Wagner and Pruß, 2002) with the valid range from 673.15 to 1273.15 K and 0 to 1.0 GPa, our EOS shows very good agreements within ±0.6% and an averaged relative deviation of about 0.1%. Compared with the accurate EOS for carbon dioxide proposed by Span and Wagner (1996) with a valid range from 673.15 to 1073.15 K and 0 to 800.0 MPa, the new EOS agrees well with deviations within ±1.0% and an averaged relative deviation of less than 0.3%. At higher temperatures and pressures from 673.15 to 2573.15 K and 1000.0 to 10.0 GPa, the new EOS accurately reproduces the simulated volumes of water with

Table 4
Parameters for the new EOS in this study (Eqs. (9) and (10))

Pressure range	Parameters	H_2O	CO_2
0–0.2 GPa	a_1	4.38269941E−02	1.14400435E−01
	a_2	−1.68244362E−01	−9.38526684E−01
	a_3	−2.36923373E−01	7.21857006E−01
	a_4	1.13027462E−02	8.81072902E−03
	a_5	−7.67764181E−02	6.36473911E−02
	a_6	9.71820593E−02	−7.70822213E−02
	a_7	6.62674916E−05	9.01506064E−04
	a_8	1.06637349E−03	−6.81834166E−03
	a_9	−1.23265258E−03	7.32364258E−03
	a_{10}	−8.93953948E−06	−1.10288237E−04
	a_{11}	−3.88124606E−05	1.26524193E−03
	a_{12}	5.61510206E−05	−1.49730823E−03
	α	7.51274488E−03	7.81940730E−03
	β	2.51598931E+00	−4.22918013E+00
	γ	3.94000000E−02	1.58500000E−01
0.2–10.0 GPa	a_1	4.68071541E−02	5.72573440E−03
	a_2	−2.81275941E−01	7.94836769E+00
	a_3	−2.43926365E−01	−3.84236281E+01
	a_4	1.10016958E−02	3.71600369E−02
	a_5	−3.86603525E−02	−1.92888994E+00
	a_6	9.30095461E−02	6.64254770E+00
	a_7	−1.15747171E−05	−7.02203950E−06
	a_8	4.19873848E−04	1.77093234E−02
	a_9	−5.82739501E−04	−4.81892026E−02
	a_{10}	1.00936000E−06	3.88344869E−06
	a_{11}	−1.01713593E−05	−5.54833167E−04
	a_{12}	1.63934213E−05	1.70489748E−03
	α	−4.49505919E−02	−4.13039220E−01
	β	−3.15028174E−01	−8.47988634E+00
	γ	1.25000000E−02	2.80000000E−02

deviations within ±1.3% and an averaged relative deviation around 0.3%. Meanwhile, the calculated volumes of carbon dioxide agree well with simulation results within −2.24% to +0.96% and the averaged relative deviation is about 0.43%.

The mixture parameters in Eq. (9) $(BV_c, CV_c^2, DV_c^4, \ldots)$ are obtained from combining the end-member parameters by the mixing rule listed in Table 5, which was suggested by (Duan et al., 1992). Three empirical mixing parameters ($k_{1,ij}$,$k_{2,ijk}$, and $k_{3,ijk}$) are included to improve the accuracies and their relationships with temperature are listed in Table 6. Compared with the simulated data for the mixture listed in the electronic annex EA-1, the developed equation of state shows remarkable accuracy with averaged deviation of 0.9%. In the mean time, our EOS reproduces over one thousand experimental data presented by Seitz and Blencoe, 1999, Shmulovich et al. (1980), Sterner and Bodnar (1991), Frost and Wood (1997), Fenghour et al. (1996), Hnedkovsky et al. (1996), Wormald et al. (1986) and Greenwood (1969) with an averaged deviation of 0.77%. Our EOS agrees with the measurements of Seitz and Blencoe (1999) at 673.15 K with an averaged deviation of less than 0.4% and maximum deviation of less than 1.5%. Compared with Sterner and Bodnar (1991), we find noticeable deviations at 973.15 K and 300.0 MPa in the water-rich region, where the maximum deviation reaches 7.71% when $x_{CO_2} = 0.3716$. However, as analyzed by Churakov and Gottschalk (2003), the experimental data of Sterner and Bodnar (1991) in this region show increasing negative excess volumes as the composition of water enhanced. Furthermore, a series of additional simulations at these conditions confirm the accuracy of our EOS with deviations around 1.0%.

With the developed EOS, the relation between the partial fugacity coefficient ϕ_i at (T, P, x_i, V), and ϕ_i^{ref} at $(T, P^{\text{ref}}, x_i, V^{\text{ref}})$ can be derived with the following formula:

$$\begin{aligned}
\ln\phi_i - \ln\phi_i^{\text{ref}} &= \ln\frac{f_i}{x_i P} - \ln\frac{f_i^{\text{ref}}}{x_i P^{\text{ref}}} \\
&= -\ln\frac{P}{P^{\text{ref}}} + \frac{1}{RT}\left(\left(\frac{\partial A(T,nV,n)}{\partial n_i}\right)_{T,nV,n_j} - \left(\frac{\partial A^{\text{ref}}(T,nV^{\text{ref}},n)}{\partial n_i}\right)_{T,nV^{\text{ref}},n_j}\right) \\
&= -\ln\frac{P}{P^{\text{ref}}} - \frac{1}{RT}\int_{V^{\text{ref}}}^{V}\left(\frac{\partial P}{\partial n_i}\right)_{T,nV,n_j} d(nV) \\
&= -\ln Z + \ln Z^{\text{ref}} + \frac{(BV_c)'}{V}\Big|_{V^{\text{ref}}}^{V} \\
&\quad + \frac{(CV_c^2)'}{2V^2}\Big|_{V^{\text{ref}}}^{V} + \frac{(DV_c^4)'}{4V^4}\Big|_{V^{\text{ref}}}^{V} \\
&\quad + \frac{(EV_c^5)'}{5V^5}\Big|_{V^{\text{ref}}}^{V} - \frac{1}{2\gamma V_c^2}(FV_c^2)' \\
&\quad \times \exp\left(-\frac{\gamma V_c^2}{V^2}\right)\Big|_{V^{\text{ref}}}^{V} - \frac{1}{2(\gamma V_c^2)^2} \\
&\quad \times \left((GV_c^4)' + (\gamma V_c^2 - (\gamma V_c^2)')FV_c^2\right) \\
&\quad \times \left(\frac{\gamma V_c^2}{V^2} + 1\right) \times \exp\left(-\frac{\gamma V_c^2}{V^2}\right)\Big|_{V^{\text{ref}}}^{V} \\
&\quad - \frac{1}{2(\gamma V_c^2)^3} \times GV_c^4 \times \left(\gamma V_c^2 - (\gamma V_c^2)'\right) \\
&\quad \times \left(\frac{(\gamma V_c^2)^2}{V^4} + \frac{2\gamma V_c^2}{V^2} + 2\right) \times \exp\left(-\frac{\gamma V_c^2}{V^2}\right)\Big|_{V^{\text{ref}}}^{V},
\end{aligned} \tag{11}$$

where f_i and f_i^{ref} are the partial fugacity, n is the total number of moles in the mixture, A and A^{ref} are Helmholtz free energies, $Z^{\text{ref}} = P^{\text{ref}}V^{\text{ref}}/RT$ is the compressibility factor at $(T, P^{\text{ref}}, V^{\text{ref}})$. The derivatives $((BV_c)', (CV_c^2)', \ldots)$ are listed in Table 5. The notations with integration limits $(\frac{(BV_c)'}{V}\big|_{V^{\text{ref}}}^{V} = \frac{(BV_c)'}{V} - \frac{(BV_c)'}{V^{\text{ref}}}\cdots)$ are adopted here for clarity.

When the pressure P is less than 0.2 GPa, the ideal gas state with $V^{\text{ref}} = \infty$, $\phi_i^{\text{ref}} = 1.0$, $Z^{\text{ref}} = 1.0$ is selected and the partial fugacity coefficient ϕ_i can be straightforwardly derived with Eq. (11). While when the pressure is larger than 0.2 GPa, we need to calculate the partial fugacity coefficient in two steps: firstly calculate the referenced partial fugacity coefficient at 0.2 GPa with the lower pressure

Table 5
Mixing rule for the EOS of the CO_2–H_2O mixture and derivatives in Eq. (11)

$BV_c = \sum_i \sum_j x_i x_j B_{ij} V_{cij}$	$B_{ij} = [(B_i^{1/3} + B_j^{1/3})/2]^3 k_{1,ij}, \quad k_{1,ij} = 1.0 (i = j)$
$(BV_c)' = 2\sum_j x_j B_{ij} V_{cij}$	$V_{cij} = [(V_{ci}^{1/3} + V_{cj}^{1/3})/2]^3$
$CV_c^2 = \sum_i \sum_j \sum_k x_i x_j x_k C_{ijk} V_{cijk}^2$	$C_{ijk} = [(C_i^{1/3} + C_j^{1/3} + C_k^{1/3})/3]^3 k_{2,ijk}, \quad k_{2,ijk} = 1.0 \ (i = j = k),$ $k_{2,iij} = k_{2,jji}$
$(CV_c^2)' = 3\sum_j \sum_k x_j x_k C_{ijk} V_{cijk}^2$	$V_{cijk} = [(V_{ci}^{1/3} + V_{cj}^{1/3} + V_{ck}^{1/3})/3]^3$
$DV_c^4 = \sum_i \sum_j \sum_k \sum_l \sum_m x_i x_j x_k x_l x_m D_{ijklm} V_{cijklm}^4$	$D_{ijklm} = [(D_i^{1/3} + D_j^{1/3} + D_k^{1/3} + D_l^{1/3} + D_m^{1/3})/5]^3$
$(DV_c^4)' = 5\sum_j \sum_k \sum_l \sum_m x_j x_k x_l x_m D_{ijklm} V_{cijklm}^4$	$V_{cijk} = [(V_{ci}^{1/3} + V_{cj}^{1/3} + V_{ck}^{1/3} + V_{cl}^{1/3} + V_{cm}^{1/3})/5]^3$
$EV_c^5 = \sum_i \sum_j \sum_k \sum_l \sum_m \sum_n x_i x_j x_k x_l x_m x_n E_{ijklmn} V_{cijklmn}^5$	$E_{ijklm} = [(E_i^{1/3} + E_j^{1/3} + E_k^{1/3} + E_l^{1/3} + E_m^{1/3} + E_n^{1/3})/6]^3$
$(EV_c^5)' = 6\sum_j \sum_k \sum_l \sum_m \sum_n x_j x_k x_l x_m x_n E_{ijklmn} V_{cijklmn}^5$	$V_{cijk} = [(V_{ci}^{1/3} + V_{cj}^{1/3} + V_{ck}^{1/3} + V_{cl}^{1/3} + V_{cm}^{1/3} + V_{cn}^{1/3})/6]^3$
$FV_c^2 = \sum_i \sum_j x_i x_j F_{ij} V_{cij}^2$	$F_{ijk} = [(F_i^{1/3} + F_j^{1/3})/2]^3$
$(FV_c^2)' = 2\sum_j x_j F_{ij} V_{cij}^2$	$V_{cij} = [(V_{ci}^{1/3} + V_{cj}^{1/3})/2]^3$
$\beta = \sum_i x_i \beta_i$	
$\beta' = \beta_i$	
$\gamma V_c^2 = \sum_i \sum_j \sum_k x_i x_j x_k \gamma_{ijk} V_{cijk}^2$	$\gamma_{ijk} = [(\gamma_i^{1/3} + \gamma_j^{1/3} + \gamma_k^{1/3})/3]^3 k_{3,ijk}, \quad k_{3,ijk} = 1.0 \ (i = j = k),$ $k_{3,iij} = k_{3,jji}$
$(\gamma V_c^2)' = 3\sum_j \sum_k x_j x_k \gamma_{ijk} V_{cijk}^2$	$V_{cijk} = [(V_{ci}^{1/3} + V_{cj}^{1/3} + V_{ck}^{1/3})/3]^3$

Table 6
The binary interaction parameters of CO_2–H_2O when 673.15 K $\leqslant T \leqslant$ 2573.15 K

Pressure range	Parameters
0–0.2 GPa	$k_1 = 3.131 - 5.0624\text{E}{-}03\ T + 1.8641\text{E}{-}06\ T^2 - 31.409/T$ $k_2 = -46.646 + 4.2877\text{E-}02\ T - 1.0892\text{E}{-}05\ T^2 + 1.5782\text{E} + 04/T$ $k_3 = 0.9$
0.2–10.0 GPa	$k_1 = 9.034 - 7.9212\text{E}{-}03\ T + 2.3285\text{E}{-}06\ T^2 - 2.4221\text{E} + 03/T$ $k_2 = -1.068 + 1.8756\text{E}{-}03\ T - \ 4.9371\text{E}{-}07\ T^2 + 6.6180\text{E} + 02/T$ $k_3 = 1.0$

parameters listed in Table 4, then replace another set of parameters valid at higher pressures and continue the calculations with Eq. (11).

With the calculated partial fugacity coefficients, it is convenient to calculate the activity a_i at (T, P, x_i) with the following equation:

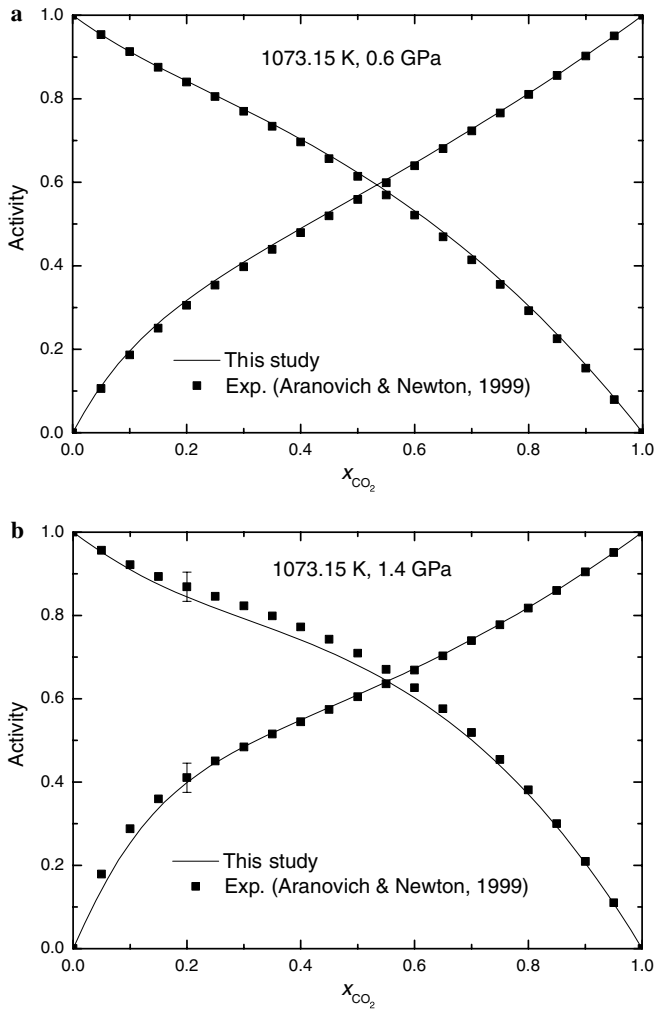

Fig. 10. Activity–concentration relations of the system CO_2–H_2O at 1073.15 K and (a) 0.6 GPa, (b) 1.4 GPa calculated from the EOS of this study (continuous curves) and those experimentally determined by Aranovich and Newton (1999) (square points). The claimed uncertainties involved in the experimental data are marked with error bars.

$$a_i = \frac{f_i}{f_i^0} = \frac{\phi_i x_i}{\phi_i^0}, \tag{12}$$

where f_i^0 and ϕ_i^0 are the fugacity and fugacity coefficient of pure component i at (T, P). Fig. 10 shows the calculated activity–composition relations at 1073.15 K and two pressures of 0.6 and 1.4 GPa, they agree with those experimentally determined by Aranovich and Newton (1999).

5. Conclusion

The CO_2–H_2O mixtures are ubiquitously typical geological fluids, but the $PVTx$ data of this system are still scarce for geological applications. To supplement the existing experimental database, with laborious and careful selection of the molecular interaction potentials, in this study we carried out more than one thousand molecular dynamics simulations of the CO_2–H_2O system. Our simulations show remarkable accuracies as demonstrated by comparison with reliable experimental data available up to high temperatures and pressures, with an average deviation of about 1.0%. The consistent and stable predictability of the simulation from low to high temperature–pressure and the fact that the molecular dynamics simulation resort to *no* experimental data but to ab initio molecular potential makes us convinced that the simulation results of the $PVTx$ properties of the CO_2–H_2O system should be reliable up to at least 2573 K and 10 GPa with errors less than 2% in density.

In order to integrate all the experimental and simulated data covering a wide temperature and pressure range with experimental accuracy for geochemical applications, we developed an equation of state for the H_2O, CO_2, and CO_2–H_2O systems valid from 673.15 to 2573.15 K and from 0 to 10.0 GPa with errors less than 2% in density. This EOS should represent the most accurate model in a very wide temperature and pressure range. From this EOS, volumetric properties (density, volumes, and excess volumes), heat properties (enthalpy), and chemical properties (fugacity, activity, chemical potential, and possibly supercritical phase separation) can be derived. A program for this EOS has been programmed and can be downloaded from the website: www.geochem-model.org/programs.htm.

Acknowledgments

Thanks to Drs. I-Ming Chou, David J. Wesolowski, and two anonymous reviewers for valuable comments. This work is supported by Zhenhao Duan's "Key Project Funds" (No. 40537032) and "Outstanding Young Scientist Funds" (No. 40225008) awarded by National Science Foundation of China. We acknowledge the generous help of Professor J. Sadlej for providing ab initio potential data of the CO_2–H_2O complex. Thanks for Dr. Jiawen Hu for providing the unpublished Fig. 1 and Table 1.

Associate editor: David J. Wesolowski

Appendix A. Supplementary data

Supplementary data associated with this article can be found, in the online version, at doi:10.1016/j.gca.2006.02.009.

References

Allen, M.P., Tildesley, D.J., 1989. *Computer Simulation of Liquids*. Oxford Science Publications.

Andersen, H.C., 1983. Rattle: a "Velocity" version of the Shake algorithm for molecular dynamics calculations. *J. Comput. Phys.* **52**, 24–34.

Aranovich, L.Y., Newton, R.C., 1999. Experimental determination of CO_2–H_2O activity–composition relations at 600–1000 °C and 6–14 kbar by reversed decarbonation and dehydration reactions. *Am. Mineral.* **84**, 1319–1332.

Block, P.A., Marshall, M.D., Pedersen, L.G., Miller, R.E., 1992. Wide amplitude motion in the water–carbon dioxide and water–acetylene complexes. *J. Chem. Phys.* **96**, 7321–7332.

Bodnar, R.J., 1985. Pressure–volume–temperature-composition (PVTX) properties of the system H_2O–NaCl at elevated temperatures and pressures. PhD. dissertation. Penn. State Univ.

Bowers, T.S., 1991. The deposition of gold and other metals—pressure-induced fluid immiscibility and associated stable isotope signatures. *Geochim. Cosmochim. Acta* **55**, 2417–2434.

Bowers, T.S., Helgeson, H.C., 1983. Calculation of the thermodynamic and geochemical consequences of nonideal mixing in the system H_2O–CO_2–NaCl on phase relations in geologic systems: equation of state for H_2O–CO_2–NaCl fluids at high pressures and temperatures. *Geochim. Cosmochim. Acta* **47**, 1247–1275.

Brodholt, J., Wood, B., 1993. Molecular dynamics simulations of the properties of CO_2–H_2O mixtures at high pressures and temperatures. *Am. Mineral.* **78**, 558–564.

Churakov, S.V., Gottschalk, M., 2003. Perturbation theory based equation of state for polar molecular fluids: II. fluid mixtures. *Geochim. Cosmochim. Acta* **67** (13), 2415–2425.

Ciccotti, G., Ferrario, M., Ryckaert, J.P., 1982. Molecular dynamics of rigid systems in cartesian coordinates: a general formulation. *Mol. Phys.* **47** (6), 1253–1264.

Crovetto, R., Wood, R.H., 1992. Solubility of CO_2 in water and density of aqueous CO_2 near the solvent critical temperature. *Fluid Phase Equilibria* **74**, 271–288.

Crovetto, R., Wood, R.H., Majer, V., 1990. Densities of $\{xCO_2 + (1 - x)$-$H_2O\}$ with $x < 0.014$ at supercritical conditions molar volumes, partial molar volumes of CO_2 at infinite dilution, and excess molar volumes. *J. Chem. Thermo.* **22** (3), 231–243.

Delhommelle, J., Mille, P., 2001. Inadequacy of the Lorentz–Berthelot combining rules for accurate predictions of equilibrium properties by molecular simulation. *Mol. Phys.* **99** (8), 619–625.

Destrigneville, C.M., Brodholt, J.P., Wood, B.J., 1996. Monte Carlo simulation of H_2O–CO_2 mixtures to 1073.15 K and 30 kbar. *Chem. Geo.* **133**, 53–65.

Drummond, S.E., Ohmoto, H., 1985. Chemical evolution and mineral deposition in boiling hydrothermal systems. *Econ. Geol.* **80**, 126–147.

Duan, Z.H., Moller, N., Weare, J.H., 1992. An equation of state for the CH_4–CO_2-H_2O system: II. mixtures from 50 to 1000 °C and 0 to 1000 bars. *Geochim. Cosmochim. Acta* **56**, 2619–2631.

Duan, Z.H., Moller, N., Weare, J.H., 1996. A general equation of state for supercritical fluid mixtures and molecular dynamics simulation of mixture *PVTX* properties. *Geochim. Cosmochim. Acta* **60**, 1209–1216.

Ellis, A.J., 1959. The solubility of carbon dioxide in water at high temperatures. *Am. J. Sci.* **257** (3), 217–234.

Ellis, A.J., Golding, R.M., 1963. The solubility of carbon dioxide above 100 °C in water and in sodium chloride solutions. *Am. J. Sci.* **261**, 47–60.

Fenghour, A., Wakeham, W.A., Watson, J.T.R., 1996. Densities of (water + carbon dioxide) in the temperature range 415 K to 700 K and pressures up to 35 MPa. *J. Chem. Thermo.* **28**, 433–446.

Franck, E.U., Todheide, K., 1959. Thermische Eigenschaften uberkritischer Mischungen von Kohlendioxyd und Wasser bis zu 750 °C und 2000 atm. *Zeitschrift fur Physikalische Chemie Neue Folge* **22**, 232–245.

Frost, D.J., Wood, B.J., 1997. Experimental measurements of the properties of H_2O–CO_2 mixture at high pressures and temperatures. *Geochimi. Cosmochim. Acta* **61**, 3301–3309.

Gehrig, M., 1980. Phasengleichgewichte und pVT-Daten ternarer Mischungen aus Wasser, Kohlendioxid und Natriumchlorid bis 3 kbar und 550 °C. Ph. D. dissertation, Hochschulverlag.

Greenwood, H.J., 1969. The compressibility of gaseous mixtures of carbon dioxide and water between 0 to 500 bars pressure and 450 °C and 800 °C. *Am. J. Sci.* **267-A**, 191–208.

Haugan, P.M., Drange, H., 1992. Sequestration of CO_2 in the deep ocean by shallow injection. *Nature* **357** (6376), 318–320.

Hebach, A., Oberhof, A., Dahmen, N., 2004. Density of water + carbon dioxide at elevated pressures: measurements and correlation. *J. Chem. Eng. Data* **49** (4), 950–953.

Hnedkovsky, L., Wood, R.H., Majer, V., 1996. Volumes of aqueous solutions of CH_4, CO_2, H_2S and NH_3 at temperatures from 298.15 K to 705 K and pressures to 35 MPa. *J. Chem. Therm.* **28** (2), 125–142.

Holloway, J.R., 1977. Fugacity and activity of molecular species in supercritical fluids. In: Fraser, D.G. (Ed.), *Thermodynamics in Geology*. D Reidel Publishing, pp. 161–181.

Hurst, G.J.B., Fowler, P.W., Stone, A.J., Buckingham, A.D., 1986. Intermolecular forces in van der Waals dimers. *Int. J. Quant. Chem.* **29**, 1223–1239.

Kerrick, D.M., Jacobs, G.K., 1981. A modified Redlich-Kwong equation for H_2O, CO_2, and H_2O–CO_2 mixtures at elevated pressures and temperatures. *Am. J. Sci.* **281**, 735–767.

Kieninger, M., Ventura, O.N., 1997. Equilibrium structure of the carbon dioxide-water complex in the gas phase: an ab initio and density functional study. *J. Mol. Struct. (Theochem)* **390**, 157–167.

King, M.B., Mubarak, A., Kim, J.D., Bott, T.R., 1992. The mutual solubilities of water with supercritical and liquid carbon dioxides. *J. Supercrit. Fluids* **5** (4), 296–302.

Kong, C.L., 1973. Combining rules for intermolecular potential parameters. II. Rules for the Lennard-Jones (12-6) potential and the Morse potential. *J. Chem. Phys.* **59**, 2464–2467.

Labotka, T.C., 1991. Chemical and physical properties of fluids. *Rev. Mineral.* **26**, 43–104.

Makarewicz, J., Ha, T.-K., Bauder, A., 1993. Potential-energy surface and large amplitude motions of the water–carbon dioxide complex. *J. Chem. Phys.* **99**, 3694–3699.

Martyna, G.J., Tobias, D.J., Klein, M.L., 1994. Constant pressure molecular dynamics algorithms. *J. Chem. Phys.* **101** (5), 4177–4189.

Mehler, E.L., 1981. Self-consistent, nonorthogonal group function approximation for polyatomic systems. II. analysis of noncovalent interactions. *J. Chem. Phys.* **74**, 6298–6306.

Navon, N., David, K.-B., Izraeli, E.S., 2004. Diamond-forming fluids. *Geochim. Cosmochim. Acta* **68** (11), A277.

Nelder, J.A., Mead, R., 1965. A simplex-method for function minimization. *Comput. J.* **7** (4), 308–313.

Nighswander, J.A., Kalogerakis, N., Mehrotra, A.K., 1989. Solubilities of carbon dioxide in water and 1 wt% NaCl solution at pressures up to 10 MPa and temperatures from 80 to 200 °C. *J. Chem. Eng. Data* **34**, 355–360.

Ohsumi, T., Nakashiki, N., Shitashima, K., Hirama, K., 1992. Density change of water due to dissolution of carbon dioxide and near-field behavior of CO_2 from a source on deep-sea floor. *Energy Convers. Manage.* **33** (5-8), 685–690.

Parkinson, W.J., De Nevers, N.J., 1969. Partial molal volume of carbon dioxide in water solutions. *Ind. Eng. Chem. Fundam.* **8** (4), 709–713.

Patel, M.R., Eubank, P.T., 1988. Experimental densities and derived thermodynamic properties for carbon dioxide–water mixtures. *J. Chem. Eng. Data* **33** (2), 185–193.

Patel, M.R., Holste, J.C., Hall, K.R., Eubank, P.T., 1987. Thermophysical properties of gaseous carbon dioxide–water mixtures. *Fluid Phase Equilib.* **36**, 279–299.

Ramboz, C., Schnapper, D., Dubessy, J., 1985. The P–V–T–X–f_{O_2} evaluation of H_2O–CO_2–CH_4-bearing fluid in a wolframite vein: Reconstruction from fluid inclusion studies. *Geochim. Cosmochim. Acta* **49** (1), 205–219.

Roedder, E., 1984. *Fluid inclusions*. Mineralogical Society of America.

Sadlej, J., Makarewicz, J., Chalasinski, G., 1998. Ab initio study of energy, structure and dynamics of the water–carbon dioxide complex. *J. Chem. Phys.* **109** (10), 3919–3927.

Seitz, J.C., Blencoe, J.G., 1997. Experimental determination of the volumetric properties and solvus relations of H_2O–CO_2 mixtures at 300–400 °C and 75–1000 bars. In: *The Fifth International Symposium on Hydrothermal Reactions*, pp. 109–112.

Seitz, J.C., Blencoe, J.G., 1999. The CO_2–H_2O system. I. Experimental determination of volumetric properties at 400 °C, 10–100 MPa. *Geochimi. Cosmochimi. Acta* **63** (10), 1559–1569.

Shmulovich, K.I., Shmonov, V.M., Mazur, V.A., Kalinichev, A.G., 1980. P–V–T and activity concentration relations in the H_2O–CO_2 system (homogeneous solutions). *Geochem. Internat.* **17**, 123–139.

Singh, J., Blencoe, J.G., Anovitz, L.M., 2000. Volumetric properties and phase relations of binary H_2O–CO_2–CH_4–N_2 mixtures at 300 °C and pressures to 1000 bars. In: Tremaine, P.R. (Ed.), *Steam, Water, and Hydrothermal Systems: Physics and Chemistry Meeting the Needs of Industry*. NRC Research Press, pp. 134–143.

Span, R., Wagner, W., 1996. A new equation of state for carbon dioxide covering the fluid region from the triple-point temperature to 1100 K at pressures up to 800 MPa. *J. Phys. Chem. Ref. Data* **25** (6), 1509–1593.

Spycher, N., Pruess, K., 2005. CO_2–H_2O mixtures in the geological sequestration of CO_2 center dot. II. Partitioning in chloride brines at 12–100 °C and up to 600 bar. *Geochim. Cosmochim. Acta* **69** (13), 3309–3320.

Sterner, S.M., Bodnar, R.J., 1991. Synthetic fluid inclusions. X: experimental determination of *P–V–T–X* properties in the CO_2–H_2O system to 6 kbar and 700 °C. *Am. J. Sci.* **291**, 1–54.

Swope, W.C., Andersen, H.C., Berens, P.H., Wilson, K.R., 1982. A computer simulation method for the calculation of equilibrium constants for the formulation of physical clusters of molecules: application to small water clusters. *J. Chem. Phys.* **76**, 637–649.

Teng, H., Yamasaki, A., Chun, M.-K., Lee, H., 1997. Solubility of liquid CO_2 in water at temperatures from 278 K to 293 K and pressures from 6.44 MPa to 29.49 MPa and densities of the corresponding aqueous solutions. *J. Chem. Therm.* **29** (11), 1301–1310.

Wagner, W., Pruß, A., 2002. The IAPWS formulation 1995 for the thermodynamic properties of ordinary water substance for general and scientific use. *J. Phys. Chem. Ref. Data* **31** (2), 387–535.

Wormald, C.J., Lancaster, N.M., Sellers, A.J., 1986. The excess molar enthalpies of $\{xH_2O + (1 - x)CO\}$(g) and $\{xH_2O + (1 - x)CO_2\}$(g) at high temperatures and pressures. *J. Chem. Thermo.* **18**, 135–147.

Zakirov, I.V., 1984. The *P–V–T* relations in the H_2O–CO_2 system at 300 and 400 °C and up to 1000 bar. *Geochem. Internat.* **21**, 13–20.

Zawisza, A., Malesinska, B., 1981. Solubility of carbon dioxide in liquid water and of water in gaseous carbon dioxide in the range 0.2–5 MPa and at temperatures up to 473 K. *J. Chem. Eng. Data* **26**, 388–391.

Zhang, Z.G., Duan, Z.H., 2002. Phase equilibria of the system methane–ethane from temperature scaling Gibbs Ensemble Monte Carlo simulation. *Geochim. Cosmochim. Acta* **66** (19), 3431–3439.

Zhang, Z.G., Duan, Z.H., 2005a. Isothermal–isobaric molecular dynamics simulations of the PVT properties of water over wide range of temperatures and pressures. *Phys. Earth Planet Interiors* **149**, 335–354.

Zhang, Z.G., Duan, Z.H., 2005b. An optimized molecular potential for carbon dioxide. *J. Chem. Phys.* **122**, 214507.

Zhang, Y.G., Frantz, J.D., 1992. Investigations of fluid properties in the CO_2–CH_4–H_2O system using synthetic fluid inclusions. *Chem. Geol.* **100** (1–2), 51–72.

Zhang, J., Zhang, X., Han, B., He, J., Liu, Z., Yang, G., 2002. Study on intermolecular interactions in supercritical fluids by partial molar volume and isothermal compressibility. *J. Supercrit. Fluids* **22** (1), 15–19.